Performance analysis of reverse osmosis, membrane distillation, and pressure-retarded osmosis hybrid processes

Jihye Kim[a], Minkyu Park[b], Ho Kyong Shon[c] and Joon Ha Kim[a,d,e,1]

a. *School of Environmental Science and Engineering, Gwangju Institute of Science and Technology (GIST), Gwangju, 500-712, Korea*
b. *Department of Chemical and Environmental Engineering, University of Arizona, Tucson, AZ 85721, USA*
c. *School of Civil and Environmental Engineering, University of Technology, Sydney, Post Box 129, Broadway, NSW 2007, Australia.*
d. *Sustainable Water Resource Technology Center, GIST, Gwangju, 500-712, Korea*
e. *Center for Seawater Desalination Plant, GIST, Gwangju, 500-712, Korea*

A Manuscript for

Desalination

[1] Corresponding author
E-mail: joonkim@gist.ac.kr; Phone: 82-62-715-3277; Fax: 82-62-715-2434

Abstract

A performance analysis of a tri-combined process that consists of reverse osmosis (RO), membrane distillation (MD), and pressure-retarded osmosis (PRO) was conducted by using numerical approaches in order to evaluate its feasibility. In the hybrid process, the RO brine is partially used as the MD feed solution, and the concentrated MD brine is then mixed with the rest of the RO brine to be considered as the PRO draw solution. Here, the brine division ratio, incoming flow rate of RO, dimensions of the MD and PRO processes, and the supply cost of the MD heat source were considered as influential parameters. Previously validated process models were employed and the specific energy consumption (SEC) was calculated to examine the performance of the RO-MD-PRO hybrid process. The simulation results confirmed that the RO-MD-PRO hybrid process could outperform stand-alone RO in terms of reducing the SEC and the environmental footprint by dilution of the RO brine in locations where free or low-cost thermal energy can be exploited. Despite the need for further investigations and pilot-tests to determine its commercial practicability, this study provides insights into future directions for water and energy nexus processes for energy efficient desalination.

Keywords: Reverse osmosis (RO), Membrane distillation (MD), Pressure-retarded osmosis (PRO), RO-MD-PRO hybrid process, Performance analysis

1. Introduction

Demands for water and energy are dramatically increasing in both developing and industrialized countries. People in developing countries suffer from a lack of access to safe drinking water and sustenance energy sources, whereas those in industrialized countries consume resources more to meet increasing standards of living [1, 2]. To relieve these water and energy scarcity issues, water and energy nexus processes, i.e., the co-generation of water and energy, have received increased attention [3]. As examples, Hosseini et al. [4] analyzed a combined gas turbine and multi stage flash (MSF) desalination system in terms of exergetic, economical, and environmental aspects, and Avrin et al. [5] compared the applicability of coal-desalination and nuclear-desalination in China. However, despite the increase in research activities into water-energy nexus processes, further developments that consider sustainable and environmental impacts are still required. In particular, a combination of pressure-retarded osmosis (PRO) and membrane distillation (MD) is thought to be a favorable candidate as a water-energy nexus process. A recent publication by Han et al.[6] for instance, experimentally investigated the performance of PRO-D hybrid process through a lab-scale system.

Investigations into PRO have resumed over the last decade due to advances in membrane technology, and have received considerable attention as a salinity gradient power (SGP) process [7]. The driving force of PRO is the chemical potential difference between a low-saline feed solution and a high-saline draw solution. Specifically, water transfers from the feed side to the draw side due to osmosis phenomena, with the increased volumetric flow used to run a turbine to generate power [8]. PRO is mostly regarded as an environmental-

friendly and sustainable energy production process that uses seawater or concentrated seawater (i.e., brine from reverse osmosis (RO)) as the draw solution, while river water or wastewater effluent is used as the feed solution [9, 10]. The fact that there are no carbon dioxide emissions and that there is less periodicity to the weather conditions make this process even more attractive [11].

In the field of desalination, MD is another process that has re-emerged in recent research, as it has the benefits of both thermal and membrane technologies. In MD, water vapor is transferred to the permeate side through a microporous hydrophobic membrane because of the vapor pressure difference. There are four types of MD configurations, categorized according to the method for activating the vapor pressure difference: direct contact MD (DCMD), air gap MD (AGMD), vacuum MD (VMD), and sweep gas MD (SGMD) [12]. The advantages of MD include the rejection rate, which theoretically reaches 100% [13], and more importantly the potential to utilize the highly concentrated water. The performance of MD is not highly affected by the concentration of the feed water, unlike other desalination processes [14], which makes it possible to use MD in the treatment of high-salinity water, such as RO brine and shale gas wastewater.

In this context, a research project entitled ‘Global MVP’ (M for MD, V for valuable resource recovery, and P for PRO; hereafter GMVP) was launched in Korea, planning to construct an RO-MD-PRO hybrid pilot plant. Here, RO, a proven and widely used technology, plays the main role to produce potable water, and MD then supports the water production while PRO is used as an energy generation or recovery process. In fact, a similar project, the ‘Mega-ton water system’ has been conducted in Japan [15]. A prototype PRO plant hybridized with RO was subsequently constructed and operated by utilizing the RO brine as the draw solution and

wastewater effluent as the feed solution. Since the utilization of MD is the biggest distinction between these two projects in terms of process schemes, the design optimization of RO, MD, and PRO use can be a critical issue.

The objective of this study is to investigate the commercial feasibility of the RO-MD-PRO hybrid process by using a numerical approach. As a scenario study, the concept of the GMVP project was adopted such that RO is the first process in the system, and is followed by MD and PRO in consecutive order. Previously validated RO, MD, and PRO numerical models were applied and combined in order to evaluate the performance of the hybrid process; the efficiency was then calculated in terms of the specific energy consumption (SEC). The effects of the division ratio of the concentrated RO brine (i.e., the brine division ratio; BDR), the plant dimension ratio of MD and PRO to RO, and the supply cost of the MD heat source were importantly considered in this study in order to explore the cost-effective design of this hybrid process.

2. Materials and methods

2.1. RO-MD-PRO hybrid process

Fig. 1 illustrates the schematic of the RO-MD-PRO hybrid process. First, seawater flows into the RO membrane as a feed water, and a certain amount of the concentrated RO brine is then utilized as the MD feed solution in order to achieve higher recovery of water. Here, the same amount of produced water from RO flows into the other side of MD membrane as a permeate solution. Finally, the concentrated MD brine and the rest of the RO brine are mixed and supplied to the PRO process as the draw solution. Pressure exchanger (PX) are utilized for both RO and PRO processes, at which to recover the RO brine pressure and also to restore the remained pressure of PRO draw solution. In this process, the division ratio of the RO brine is

critical, i.e., the brine division ratio (BDR), and consists of the flow rate of the MD feed solution (denoted as x) and that of RO brine (denoted as y) (see Eq. (1)). In Fig. 1, $\dot{W}_{pump,RO}$, $\dot{W}_{heat,MD}$, $\dot{W}_{pump,PRO}$, and $\dot{W}_{p,PRO}$ indicate the rate of work done by the RO pump, MD heater, and PRO pump, and the energy generated by PRO, respectively. In addition, $Q_{p,RO}$ and $Q_{p,MD}$ are the volumetric flow rates of the RO and MD water production. The relationship among the terms will be described in detail in the following section. In the hybrid process, it is assumed that secondary wastewater effluent is used as the PRO feed solution [10], and the energy generated by PRO supports the operation of the hybrid process such that the total energy consumption can be decreased. In addition, from the four MD configurations, DCMD is applied due to its simplicity and frequent appearances in literature [14, 16].

$$\text{Brine division ratio (BDR)} = \frac{\text{Flow rate of MD feed solution } (Q_{f,MD})}{\text{Flow rate of RO brine } (Q_{b,RO})} \quad (1)$$

[Fig. 1]

2.2. RO model

Water in RO is transported through a semi-permeable membrane because the hydraulic pressure is higher than the osmotic pressure, which can be explained by the solution diffusion model [17]:

$$v_w = A(\Delta P_{RO}(x) - \Delta\pi_{RO}(x)) \quad (2)$$

where v_w is the permeate flux, A is the water permeability coefficient, ΔP_{RO} is the hydraulic pressure applied in RO, and $\Delta\pi_{RO}$ is the osmotic pressure difference across the RO membrane. The hydraulic resistance of the channel walls and spacers cause a decrease of

the hydraulic pressure along the channel, as expressed in Eq. (3) [18].

$$\Delta P_{RO}(x) = \Delta P_{RO}(x=0) - \frac{12K\mu}{H^2}\int_0^x u(\xi)d\xi \quad (3)$$

where K is the friction coefficient, μ is the dynamic viscosity of the feed water, H is the channel height, and u is the cross-flow velocity of the feed water. Concentration polarization (CP) phenomena cannot be avoided in this membrane process, causing the diminish of driving force, therefore the model which reflects CP phenomena under the existence of the spacers was employed [19, 20].

$$c_W = c_0 + e^{-v_W(x)H/D_{hd}}\frac{r_j c_0}{uH}\int_0^x v_W(\xi)d\xi + \frac{r_j c_0 v_W(x)}{uD_{hd}}\int_0^x v_W(\xi)d\xi \quad (4)$$

where c_W is the salt concentration of membrane wall, c_0 is the bulk concentration, D_{hd} is the hydraulic dispersion coefficient, and r_j is the rejection rate.

2.3. MD model

When the water vapor molecules penetrate through the MD membrane, heat and mass transfers occur concurrently, however, the heat transfer across the boundary layers functions as the dominant step, as described in the following equations [21, 22]:

$$q_f = h_f(T_f - T_{mf}) \quad (5)$$

$$q_p = h_p(T_{mp} - T_p) \quad (6)$$

$$q_m = J\Delta H + h_m(T_{mf} - T_{mp}) \quad (7)$$

where q is the heat flux, h is the heat transfer coefficient, T is the temperature, J is the mass flux across the membrane, and ΔH is the latent heat of water. The subscripts f, p, and m indicate the feed side, permeate side, and membrane, respectively. Under steady state conditions, the three heat fluxes can be equal based on principle pertaining to the

conservation of energy [21].

The mass transfer can be described as a linear function of the vapor pressure difference between the feed and permeate sides, referred to as the dusty gas model [12].

$$J = C_m(p_{mf} - p_{mp}) = C_m[p^0(T_{mf}, c_{mf}) - p^0(T_{mp}, c_{mp})] \quad (8)$$

where C_m is the mass transfer coefficient, p is the vapor pressure, and $p^0(T,c)$ is the vapor pressure of the substance at a temperature T and a concentration c. The Antoine equation and the correlations can be used to estimate the vapor pressure of feed and permeate solutions [23, 24]. The mass transfer coefficient C_m reflecting the combined Knudsen and molecular diffusion mechanisms can be expressed as [25]:

$$C_m = \frac{\varepsilon}{\tau\delta}\frac{M}{RT_{ave}}\left(\frac{1}{D_k} + \frac{p_a}{pD_{wa}}\right)^{-1} \quad (9)$$

$$T_{avg} = \frac{T_{mf} + T_{mp}}{2} \quad (10)$$

$$D_k = \frac{2}{3}r\sqrt{\frac{8RT_{ave}}{\pi M}} \quad (11)$$

$$pD_{wa} = 4.46\times10^{-6}T_{avg}^{2.334} \quad (12)$$

where C_m is the mass transfer coefficient, and Δp is the vapor pressure difference across the membrane. The Greek letters ε, τ, and δ refer to the porosity, tortuosity, and thickness of membrane, respectively. In addition, M is the molar weight of water, R is the gas constant, T_{ave} is the average temperature of the feed and permeate membrane surface, D_k is the Knudsen diffusion coefficient, r is the pore radius, D_{wa} is the molecular diffusion coefficient, and p_a is the air pressure.

In the RO-MD-PRO hybrid process, the RO brine is utilized as the MD feed solution; therefore, the effect of CP should be considered as in the case of RO. Assuming the 100% rejection rate of MD membrane and applying the film theory, CP can be expressed as follows [26]:

$$\frac{c_{mf}}{c_f} = \exp\left(\frac{J}{k_c \rho}\right) \tag{13}$$

where c_{mf} is the concentration of the membrane surface facing the feed solution, c_f is the bulk concentration of the feed solution, k_c is the mass transfer coefficient, and ρ is the density of the feed solution. In addition, changes of thermos-physical properties such as thermal conductivity, heat capacity, density and viscosity due to the presence of salt in the feed solution were considered [24]. Then, in order to simulate a large-scale system, the spatial variation of the concentration and cross-flow was considered; further explanations on how to numerically solve the equations will be provided in Section 2.5.

2.4. PRO model

The driving force of PRO is negatively affected by both the internal CP (ICP) and external CP (ECP). Changing the hydraulic conditions such as by increasing the cross-flow velocity can partially help minimize the ECP. However, the mitigation of ICP phenomena is almost impossible since enhanced mixing has little influence inside the support layer. The permeate water flux obtained by considering the ICP is described as Eq. (14), which is derived from the solute mass balance [27].

$$v_w = \frac{D}{S}\ln\left(\frac{B(c_a - c_i) + v_w c_i}{B(c_a - c_i) + v_w c_{b,\,feed}}\right) \tag{14}$$

where D is the diffusivity coefficient of the solute, S is the membrane structure parameter, B

is the solute permeability coefficient, c_a is the concentration at the active layer surface, c_i is the concentration at the active layer and support layer interface, and $c_{b,feed}$ is the concentration of the bulk feed solution. Due to the existence of ECP, c_a is not equal to $c_{b,feed}$, and can be expressed as Eq. (13), based on the film theory [28]:

$$c_a = c_{b,draw} \exp(-\frac{v_w}{k}) \tag{15}$$

where $c_{b,draw}$ is the concentration of the draw solution in the bulk region, and *k* is the mass transfer coefficient. Substituting Eq. (14) into Eq. (13) becomes

$$v_w = \frac{D}{S} \ln\left(\frac{B(c_{b,draw} \exp(-\frac{v_w}{k}) - c_i) + v_w c_i}{B(c_{b,draw} \exp(-\frac{v_w}{k}) - c_i) + v_w c_{b,feed}} \right). \tag{16}$$

In addition, the spatial distributions of the concentration and cross-flow velocity along the channel were employed in order to simulate a practical large-scale process [29].

2.5. Modelling procedure

Fig. 2 illustrates the flow chart used to evaluate the performance of the RO-MD-PRO hybrid process. Simulations of the RO, MD, and PRO processes were conducted in consecutive order and the specific energy consumption (SEC) was calculated at the end of each process. Here, only the procedure for the MD simulation is introduced in further detail, since the procedures for the RO and PRO processes can be found elsewhere [29].

In the MD process, it is not possible to measure the concentration and temperature at the membrane surface, resulting in the need to obtain arbitrary initial values of T_{mf} and c_{mf}. These initial values were then used to calculate the average temperature T_{ave} according to

Eqs. (4), (5), and (9). The updated values of T_{mf} and c_{mf} were obtained by solving Eqs. (6), (7), and (12), and the updated values were then replaced with the previously estimated values. This iteration procedure was repeated until the error value met the criterion.

After each simulation of the hybrid processes was completed, the SEC was calculated using Eq. (16). The SEC is widely used in stand-alone RO processes as the relation between energy consumption and water production [30]; therefore, the equation was slightly modified to reflect the characteristics of the RO-MD-PRO hybrid process.

$$SEC = \frac{(\dot{W}_{pump,RO} + \dot{W}_{heat,MD} + \dot{W}_{pump,PRO} - \dot{W}_{p,PRO})}{Q_{p,RO} + Q_{p,MD}} \tag{17}$$

$$\dot{W}_{pump,RO} = \Delta P_{RO}\left(Q_{f,RO} - \eta_{PX,RO} Q_{b,RO}\right) \tag{18}$$

$$\dot{W}_{heat,MD} = C_p V_f \rho_f (T_{f,MD} - T_{b,RO}) \tag{19}$$

$$\dot{W}_{pump,PRO} = \Delta P_{PRO} Q_{d,PRO}\left(1 - \eta_{PX,PRO}\right) \tag{20}$$

$$\dot{W}_{p,PRO} = \eta_{turbine,PRO} Q_{p,PRO} \Delta P_{PRO} \tag{21}$$

where $Q_{f,RO}$ is the volumetric flow rate of RO feed water, $Q_{b,RO}$ is the volumetric flow rate of RO brine, $\eta_{PX,RO}$ is the PX efficiency of RO, C_p is the heat capacity, V_f is the volumetric flow rate of MD feed solution, ρ_f is the density of MD feed solution, $T_{f,MD}$ and $T_{b,RO}$ are the temperatures of MD feed solution and RO brine, ΔP_{PRO} is the applied hydraulic pressure of PRO, $Q_{d,PRO}$ is the volumetric flow rate of PRO draw solution, $\eta_{PX,PRO}$ is the PX efficiency of PRO, $\eta_{turbine,PRO}$ is the efficiency of hydro-turbine for PRO, $Q_{p,PRO}$ is the volumetric flow rate of permeated water in PRO. It should be noted that the energy required to chill the MD permeate solution was not considered in the current study assuming the identical temperatures for RO and MD permeate side.

[Fig. 2]

2.6. Simulation conditions

The conditions used to simulate the hybrid process are summarized in Table 1. The concentration of the MD feed solution remains steady at about 76 g/L NaCl in most cases, resulting from the no change in RO feed concentrations; there are slight variations shown in Section 3.2 when different RO influent flow rates were applied. However, the concentration of the PRO draw solution continually varied according to the BDR. In both MD and PRO, the streams flowing on each side of the membranes have identical flow rates (i.e., feed and permeate solutions for MD and draw and feed solutions for PRO). As the influent flow of MD feed solution and PRO draw solution is restricted by the amount of RO brine, the RO plant should be larger than the MD and PRO plants; assume here that the dimensions of the MD and PRO plants are half of the RO plants unless otherwise mentioned (Section 3.3). To avoid the underestimation of other parameters caused by the dominant effect of the MD heat cost, it was also assumed that renewable energy or low-grade heat can be complimentarily utilized, except incorporating the required energy to heat feed solution (Section 3.4). In the whole simulations, however, cooling cost for the MD permeate solution was excluded due to the assumption of identical temperature at RO and MD permeate side. The Van't Hoff equation was used to calculate the osmotic pressure in RO and PRO, and the membrane properties of each process were obtained from previous literature [8, 18, 31].

[Table 1]

2.7. Sensitivity analysis

Latin hypercube (LH) sampling and the one-factor-at-a-time (OAT) method (denoted as LH-OAT) was employed to determine the dominant parameters on the performance of the RO-MD-PRO hybrid process, from among the influential parameters. For the sensitivity analysis, seven input parameters were used, which included: the pressure applied in RO, cross-flow velocity of RO, BDR, cost sharing ratio of MD heat source, concentration of PRO feed solution, pressure applied in PRO, and plant dimension ratio of MD and PRO compared to RO plant. Note that linked parameters such as the cross-flow velocity of MD and PRO, and concentrations of the MD feed and PRO draw solutions, which are concurrently the output of the prior processes and inputs of the following processes, were not considered. In the LH-OAT method, the sensitivity analysis is performed in a loop, with the beginning point of each loop being set by the LH sampling. Then, a partial effect for parameter ($S_{i,j}$) around LH sample point j could be calculated using Eq. (17) [32, 33].

$$S_{i,j} = \frac{100\left(\left|\frac{M(\Phi_1,...,\Phi_i(1+f),...,\Phi_p) - M(\Phi_1,...,\Phi_i,...,\Phi_p)}{[M(\Phi_1,...,\Phi_i(1+f),...,\Phi_p) + M(\Phi_1,...,\Phi_i,...,\Phi_p)]/2}\right|\right)}{f} \quad (17)$$

where *M* is the model function of the SEC, f indicates the fraction by which the parameter is changed, and Φ_i and Φ_p denote each parameter and the final parameter, respectively. The average of the partial effect of each loop is regarded as the sensitivity value. Therefore, the most dominant parameters of the RO-MD-PRO hybrid process are those having the highest sensitivity value.

3. Results and discussion

3.1. Performance of the stand-alone RO process

For a comparison, the performance simulation of a stand-alone RO process was conducted under the given conditions in Table 1 and the results were summarized in Table 2. In brief,

the recovery rate was 49.7%, i.e., the water production and brine flow rate were 995 m^3/d and 1005 m^3/d, respectively. The SEC was approximately 1.914 kWh/m^3, which represents the efficiency of the stand-alone RO process.

[Table 2]

3.2. Influence of BDR

In the RO-MD-PRO hybrid process, influent conditions of the MD and PRO processes such as concentration and the flow rate are dependent on the BDR (i.e., x/y in Eq. (1)). To investigate the impact of BDR on the hybrid process performance, we varied the BDR values from 0.0 to 1.0. For example, if the BDR equals 0.1, 10% of the RO brine flows into the MD feed side, whereas all the RO brine is utilized as the MD feed solution when the BDR is equal to 1.0. The RO-PRO hybrid process with no MD is expressed as BDR equals 0.

As can be seen in Fig. 3(a), the recovery rate did not vary much, especially at the lower BDR values, because it solely depends on the total amount of water produced. Since water production is not a primary MD contribution, but rather RO, the recovery rate remained similar unless the influent flow rate was varied, resulting in a recovery rate increase of approximately 5% that was obtained by increasing the BDR values. Furthermore, the effect of BDR on the performance of the hybrid process in terms of the SEC and power generation is shown in Fig. 3(b). If the BDR value is increased, the driving force of PRO increased by obtaining a higher portion of the concentrated MD brine than RO brine, eventually leading to a decrease of the SEC in the hybrid process. A maxiumum SEC was ~1.6 at a BDR of 1.0, which was a 17% reduction compared to the stand-alone RO process. It is worth pointing out that the SEC sharply decreased even at a BDR of 0, which is the RO-PRO hybrid.

[Fig. 3]

3.3. Influence of RO influent flow rate

The MD and PRO flow rates significantly depend on the influent flow rate from RO. Hence, the impact of RO influent was investigated by varying the feed flow rate from 2000 m^3/d to 6000 m^3/d.

Fig. 4 compares the SECs at various RO influent flow rates, in which an increase in the influent flow has a negligible effect on the SEC in the stand-alone RO. However, there is a striking difference in the hybrid processes, for both RO-PRO and RO-MD-PRO. Regardless of the RO influent flow rate, the SEC decreased with an increase in the BDR, as described in the previous section. Interestingly, the extent of SEC decrease from the feed flow rate 4000 m^3/d to 2000 m^3/d was larger than that from 6000 m^3/d to 4000 m^3/d. The low SEC at the lower RO influent flow rate (2000 m^3/d) would be due to there being a lower energy consumption to drive the PRO draw solution.

[Fig. 4]

The concentration of the RO brine ranged from 74 g/L to 76 g/L at various incoming flow rates. Therefore, direct discharge without attenuation of the salt content would adversely influence the receiving water bodies. In addition to the SEC reduction, the second advantage of utilizing a hybrid process lies in the dilution effect of the concentrated RO brine. As can be seen in Fig. 5, it is clear that the hybrid process has high potential to dilute the RO brine. Specifically, a maximum of 50% dilution was achieved in the BDR of 0 (i.e., RO-PRO

hybrid configuration), and the effect then slightly decreased with a further BDR increase, resulting from the more concentrated incoming draw solution for PRO. Moreover, varying the RO influent flow rate did not significantly influence the water quality of the final discharge.

[Fig. 5]

3.4. Influence of MD and PRO plant dimension

Due to the consecutive order processed, the dimension of the ratio between process sequences can be an important parameter for determining the efficiency of the hybrid process. In addition, the effects of RO plant dimension can propagate through both the MD and PRO processes. Therefore, to verify the effect of plant dimensions, we varied the dimension of MD and PRO plants from 10% to 60% relative to the RO plants, and then estimated the SEC and concentration of the final discharge. The maximum dimension of the MD and PRO plants was restricted to 60% of the RO to ensure that a sufficient amount of water was provided to these plants.

The impact of dimension variation of the MD and PRO plants on the SEC at BDR values of 0.1, 0.5, and 1.0 is expressed in Fig. 6. At a BDR of 0.1, the SEC is primarily dependent on the PRO plant dimension. For example, the energy consumption is minimized by increasing the PRO plant because the increase in energy generated by PRO. Meanwhile, if the PRO plant dimension is fixed, the SEC is only varied by the energy generation of PRO ($\dot{W}_{p,PRO}$) and water production of MD ($Q_{p,MD}$), as can be seen in Eq. (16). Additional water production can be obtained by increasing the MD plant dimension. However, any reduction in the

volumetric flow of PRO draw solution causes a decrease in the energy generation of PRO. As the PRO energy generation has a greater influence than the water production by MD, increasing the MD plant dimension results in a negative impact on the SEC. No significant variation of SEC was observed by changing the MD plant dimension when the BDR equals 0.5. However, it was found that the dimension of both MD and PRO plants almost equivalently influenced the SEC at a BDR value of 1.0; the entire amount of RO brine flow was initially utilized as MD feed solution, thus the performance of PRO was directly determined by the conditions of MD outflow.

[Fig. 6]

3.5. Influence of supply cost of MD heat source

Despite the importance of the MD heat supply, it was assumed that the required energy in MD can be supplied free of charge in the previous sections in order to prevent an underestimation of other parameters influencing the hybrid process. In reality, however, the supply conditions of the MD heat source can be determined by the geographical location, i.e., the energy cost and the potential to utilize the waste heat are highly reliant on local policies and the market economy in specific countries. Therefore, we considered three scenarios by varying the cost of the MD heat supply: 1) utilization of the MD heat source for free, 2) 5% cost sharing of the MD heat cost, and 3) 10% cost sharing of the MD heat cost. The cost sharing ratio was limited up to 10% because the results are already economically unfavorable.

Fig. 7 illustrates the effect of MD heat supply cost at various BDRs. The SEC ranged from 1.61 kWh/m^3 to 1.78 kWh/m^3 under the scenario that free energy is available. However, it dramatically increased if the supply cost needs to be paid. Further increases of the SEC were

observed according to increases in the BDR because more energy was required to heat the increased MD flow rates. Similar to this assumption, it was demonstrated that the expense of the MD heat supply dominantly influenced the performance of the hybrid process. Therefore, the utilization of a free heat source such as waste heat is strongly desired in order to apply MD in a commercial-scale hybrid plant.

[Fig. 7]

3.6. Sensitivity analysis of influential parameters

A sensitivity analysis was conducted to identify influential performance parameters based on the SEC of the RO-MD-PRO hybrid process. The employed simulation conditions are as follows: for RO, the applied pressure ranged from 40 bar to 70 bar, and the cross-flow velocity was 0.05 m/s to 0.13 m/s. The temperature difference between the MD feed and permeate solutions ranged from 20 ℃ to 50 ℃, while in PRO, the feed concentration ranged from 0.5 g/L to 2.5 g/L and applied pressures from 15 bar to 30 bar were applied. The BDR and cost sharing ratio of the MD heat source were both varied from 0 to 1, and the PRO and MD plant dimension s was varied from 10% to 70% of that for RO.

The ranking of sensitivity index of each influential parameter is shown in Table 3. The cost sharing ratio of MD heat source ranked the first, indicating that energy required for MD significantly influences the total energy consumption in the hybrid process, as was discussed in Section 3.4. The sensitivity index also confirmed the importance of BDR. The parameters relevant to RO, including hydraulic pressure and cross-flow velocity, had a relatively high rank, suggesting that RO plays a main role in this hybrid process due to its location and plant dimension; located prior to the other processes and has larger dimensions. More importantly,

the results of the sensitivity analysis suggested that further optimization of specific parameters is critical in order to make the RO-MD-PRO hybrid process more favorable.

[Table 3]

4. Conclusions

The RO-MD-PRO hybrid process was introduced as a novel design for a water-energy nexus process and its feasibility was investigated by numerical approaches. Various influencing parameters were considered, including: the BDR, influent flow rate of RO, dimensions of MD and PRO processes, and supply cost of the MD heat source, with the performance of the hybrid process then evaluated using a modified SEC equation. The main conclusions drawn were as follows:

- The RO-MD-PRO hybrid process can outperform a stand-alone RO process in terms of its ability to reduce the SEC and mitigate harmful impacts on the marine environment caused by concentrated RO brine. Further increases in the process efficiency can be obtained by re-using the final discharge water of the hybrid system as the feed water of RO instead of simply discharging it into the sea.
- Increases in the BDR positively influence the efficiency of the hybrid process by increasing the water production by MD and the energy generation of PRO due to the higher osmotic pressure difference, which corresponds to the driving force of PRO.
- The effect of the influent flow rate of RO was not significant in the final discharge concentration, though it was in the SEC. Lowering the feed flow rate reduced the SEC, indicating that an investigation of the optimal influent conditions is still

required.

- At lower BDR values, the SEC was significantly influenced by the PRO plant dimension. However, both the MD and PRO plant dimensions almost equally influence the efficiency of the hybrid process as the BDR is increased, resulting from the increasing contribution of the MD process.
- The supply cost of the MD heat source plays a dominant role in determining the efficiency of the hybrid process. If the required energy consumed cannot be reimbursed, the RO-MD-PRO hybrid configuration will be unfavorable for any BDR value. Therefore, it is recommended to utilize the RO-MD-PRO hybrid process in locations where free or low-cost thermal energy can be exploited.

Acknowledgements

This study was supported by a project from the Global Ph.D. Fellowship, which the National Research Foundation of Korea conducted from 2011, and a grant (code 13IFIP-B065893-01) from the Industrial Facilities and Infrastructure Research Program funded by the Ministry of Land, Infrastructure, and Transport of the Korean government, and an ARC Future Fellowship.

References

[1] M.A. Shannon, P.W. Bohn, M. Elimelech, J.G. Georgiadis, B.J. Mariñas, A.M. Mayes, Science and technology for water purification in the coming decades, Nature, 452 (2008) 301-310.
[2] N. Paranychianakis, M. Salgot, S. Snyder, A. Angelakis, Water Reuse in EU-States: Necessity for Uniform

Criteria to Mitigate Human and Environmental Risks, Critical Reviews in Environmental Science and Technology, (2014) 00-00.
[3] J. Pittock, K. Hussey, S. Dovers, Climate, Energy and Water, Cambridge University Press, 2015.
[4] S.R. Hosseini, M. Amidpour, S.E. Shakib, Cost optimization of a combined power and water desalination plant with exergetic, environment and reliability consideration, Desalination, 285 (2012) 123-130.
[5] A.-P. Avrin, G. He, D.M. Kammen, Assessing the impacts of nuclear desalination and geoengineering to address China's water shortages, Desalination, 360 (2015) 1-7.
[6] G. Han, J. Zuo, C. Wan, T.-S. Chung, Hybrid Pressure Retarded Osmosis− Membrane Distillation (PRO− MD) Process for Osmotic Power and Clean Water Generation, Environmental Science: Water Research & Technology, (2015).
[7] F. Helfer, C. Lemckert, Y.G. Anissimov, Osmotic power with Pressure Retarded Osmosis: Theory, performance and trends–A review, Journal of Membrane Science, 453 (2014) 337-358.
[8] A. Achilli, T.Y. Cath, A.E. Childress, Power generation with pressure retarded osmosis: An experimental and theoretical investigation, Journal of membrane science, 343 (2009) 42-52.
[9] T. Thorsen, T. Holt, The potential for power production from salinity gradients by pressure retarded osmosis, Journal of Membrane Science, 335 (2009) 103-110.
[10] C.F. Wan, T.-S. Chung, Osmotic power generation by pressure retarded osmosis using seawater brine as the draw solution and wastewater retentate as the feed, Journal of Membrane Science, (2015).
[11] J. Kim, J. Lee, J.H. Kim, Overview of pressure-retarded osmosis (PRO) process and hybrid application to sea water reverse osmosis process, Desalination and Water Treatment, 43 (2012) 193-200.
[12] E. Curcio, E. Drioli, Membrane distillation and related operations—a review, Separation and Purification Reviews, 34 (2005) 35-86.
[13] K. Schneider, W. Hölz, R. Wollbeck, S. Ripperger, Membranes and modules for transmembrane distillation, Journal of membrane science, 39 (1988) 25-42.
[14] F. Laganà, G. Barbieri, E. Drioli, Direct contact membrane distillation: modelling and concentration experiments, Journal of membrane science, 166 (2000) 1-11.
[15] K. Saito, M. Irie, S. Zaitsu, H. Sakai, H. Hayashi, A. Tanioka, Power generation with salinity gradient by pressure retarded osmosis using concentrated brine from SWRO system and treated sewage as pure water, Desalination and Water Treatment, 41 (2012) 114-121.
[16] H.J. Hwang, K. He, S. Gray, J. Zhang, I.S. Moon, Direct contact membrane distillation (DCMD): Experimental study on the commercial PTFE membrane and modeling, Journal of Membrane Science, 371 (2011) 90-98.
[17] J. Wijmans, R. Baker, The solution-diffusion model: a review, Journal of membrane science, 107 (1995) 1-21.
[18] Y.G. Lee, Y.S. Lee, M. Park, D.R. Yang, J.H. Kim, A fouling model for simulating long-term performance of SWRO desalination process, Journal of Membrane Science, 401 (2012) 282-291.
[19] J. Schwinge, P. Neal, D. Wiley, D. Fletcher, A. Fane, Spiral wound modules and spacers: review and analysis, Journal of membrane science, 242 (2004) 129-153.
[20] W. Zhou, L. Song, T.K. Guan, A numerical study on concentration polarization and system performance of spiral wound RO membrane modules, Journal of membrane science, 271 (2006) 38-46.
[21] M. Qtaishat, T. Matsuura, B. Kruczek, M. Khayet, Heat and mass transfer analysis in direct contact membrane distillation, Desalination, 219 (2008) 272-292.
[22] J. Phattaranawik, R. Jiraratananon, A. Fane, Heat transport and membrane distillation coefficients in direct contact membrane distillation, Journal of membrane science, 212 (2003) 177-193.
[23] M. Abbott, J. Smith, H. Van Ness, Introduction to chemical engineering thermodynamics, McGraw-Hill, 2001.
[24] M.H. Sharqawy, J.H. Lienhard, S.M. Zubair, Thermophysical properties of seawater: a review of existing correlations and data, Desalination and Water Treatment, 16 (2010) 354-380.
[25] F. Suárez, S.W. Tyler, A.E. Childress, A theoretical study of a direct contact membrane distillation system coupled to a salt-gradient solar pond for terminal lakes reclamation, water research, 44 (2010) 4601-4615.
[26] Y. Yun, R. Ma, W. Zhang, A. Fane, J. Li, Direct contact membrane distillation mechanism for high concentration NaCl solutions, Desalination, 188 (2006) 251-262.
[27] K. Lee, R. Baker, H. Lonsdale, Membranes for power generation by pressure-retarded osmosis, Journal of Membrane Science, 8 (1981) 141-171.
[28] E.M. Hoek, A.S. Kim, M. Elimelech, Influence of crossflow membrane filter geometry and shear rate on colloidal fouling in reverse osmosis and nanofiltration separations, Environmental Engineering Science, 19 (2002) 357-372.
[29] J. Kim, M. Park, S.A. Snyder, J.H. Kim, Reverse osmosis (RO) and pressure retarded osmosis (PRO) hybrid processes: model-based scenario study, Desalination, 322 (2013) 121-130.

[30] A. Zhu, P.D. Christofides, Y. Cohen, Energy consumption optimization of reverse osmosis membrane water desalination subject to feed salinity fluctuation, Industrial & Engineering Chemistry Research, 48 (2009) 9581-9589.
[31] G. Naidu, S. Jeong, S. Vigneswaran, Influence of feed/permeate velocity on scaling development in a direct contact membrane distillation, Separation and Purification Technology, 125 (2014) 291-300.
[32] K. Holvoet, A. van Griensven, P. Seuntjens, P. Vanrolleghem, Sensitivity analysis for hydrology and pesticide supply towards the river in SWAT, Physics and Chemistry of the Earth, Parts A/B/C, 30 (2005) 518-526.
[33] A. Van Griensven, T. Meixner, S. Grunwald, T. Bishop, M. Diluzio, R. Srinivasan, A global sensitivity analysis tool for the parameters of multi-variable catchment models, Journal of hydrology, 324 (2006) 10-23.

Figure captions

Fig. 1. Schematic of RO-MD-PRO hybrid process with seawater as the RO feed water and wastewater effluent as the PRO feed solution.

Fig. 2. Flow chart of the RO-MD-PRO hybrid modelling procedures.

Fig. 3. Comparison of RO-MD-PRO hybrid process performances at various BDRs: (a) total water production and recovery rate, and (b) SEC and power production.

Fig. 4. Effect of RO influent flow rate on the SEC at various BDRs.

Fig. 5. Effect of RO influent flow rate on the concentration of final discharge water at various BDRs.

Fig. 6. Effect of MD and PRO plant size on the SEC at various BDRs: (a) BDR=0.1, (b) BDR=0.5, and (c) BDR=1.0.

Fig. 7. Effect of MD heat supply cost at various BDRs.

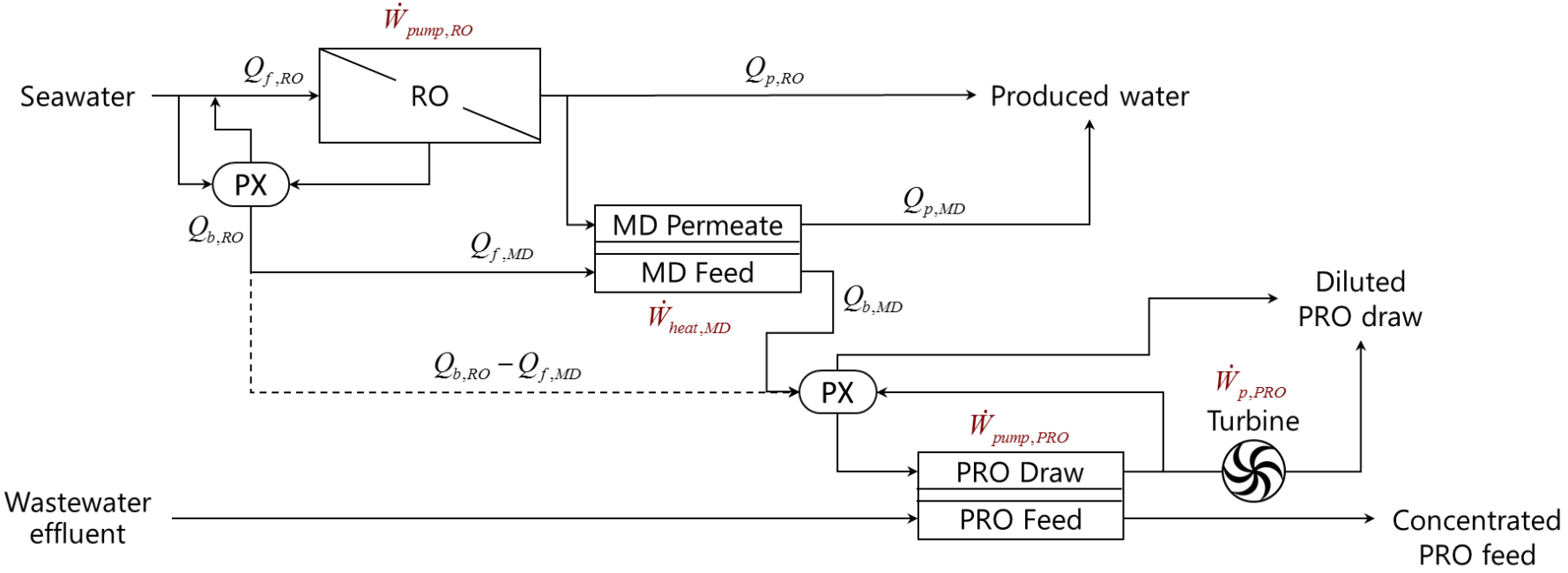

Fig. 1.

Kim *et al.*

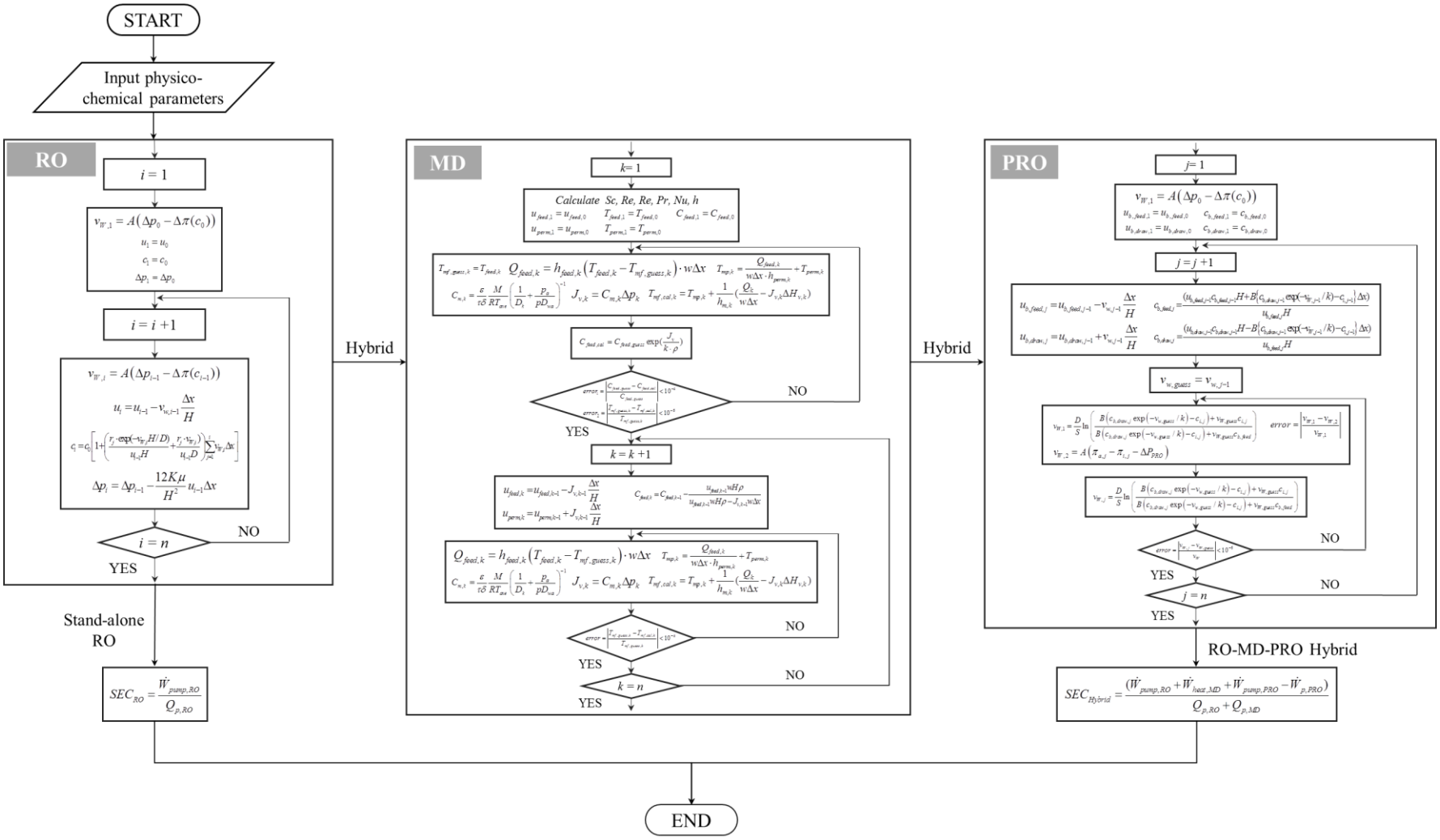

Fig. 2.

Kim *et al*.

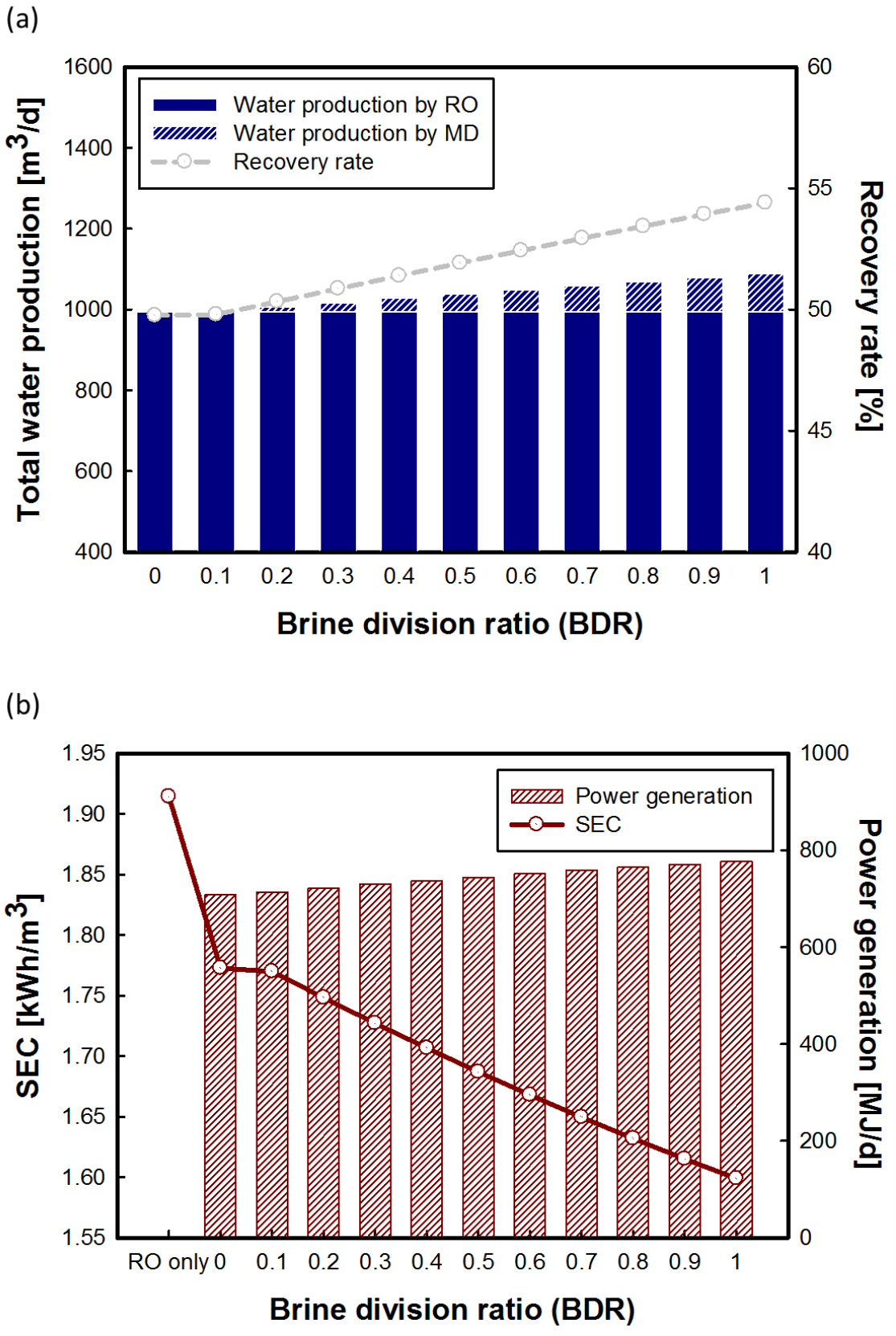

Fig. 3.

Kim *et al.*

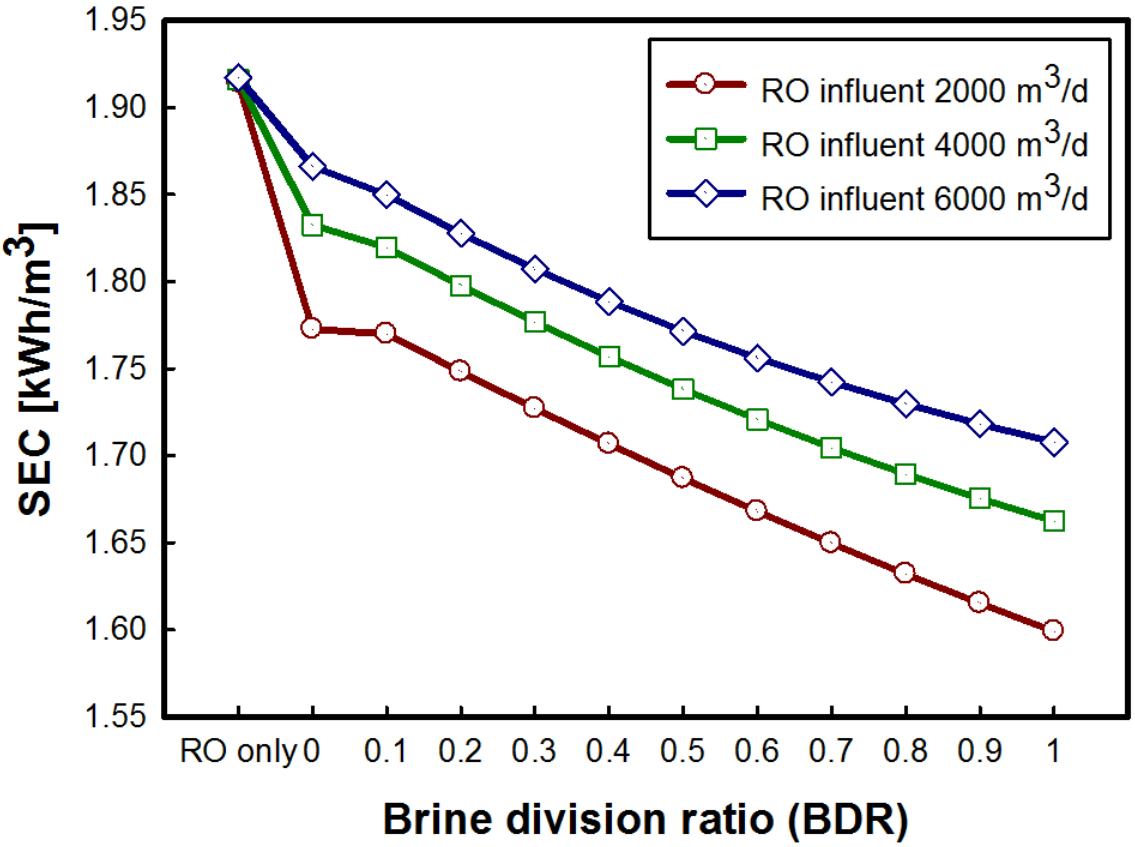

Fig. 4.

Kim *et al*.

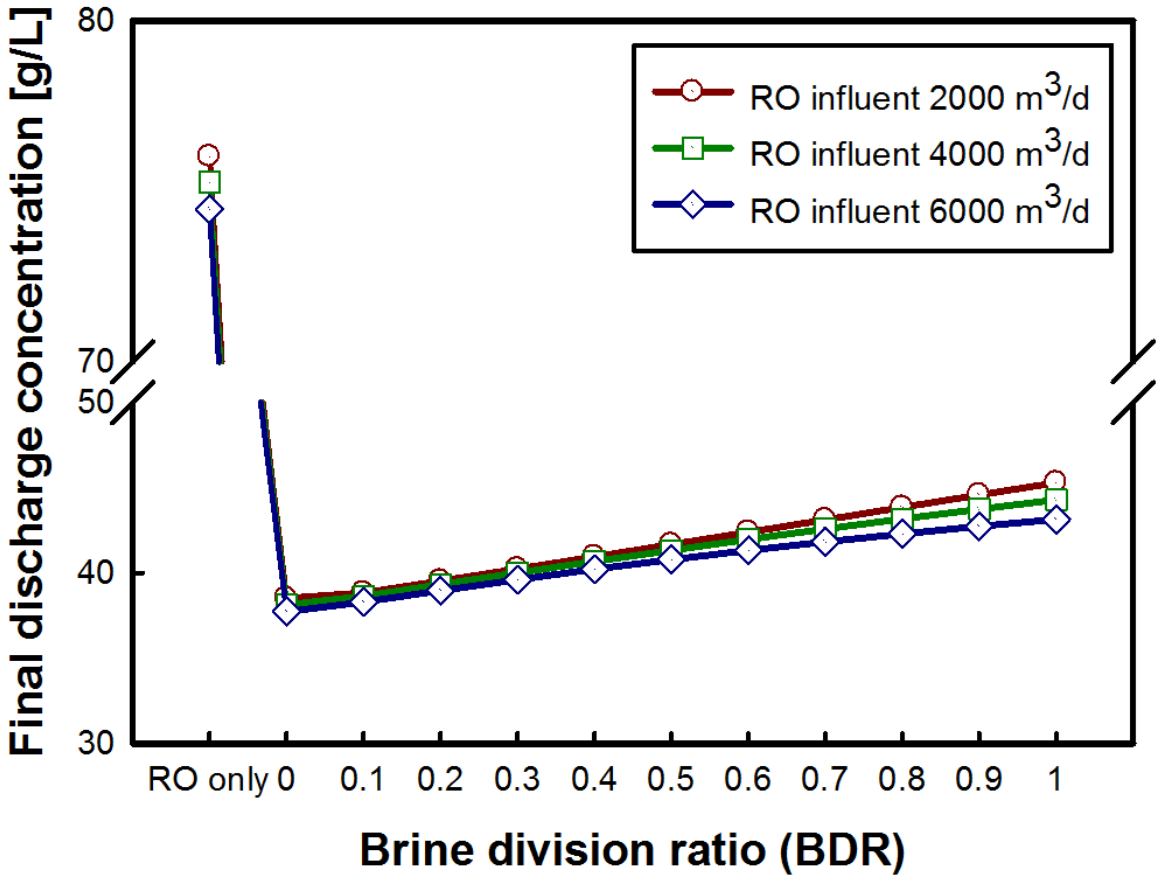

Fig. 5.

Kim *et al.*

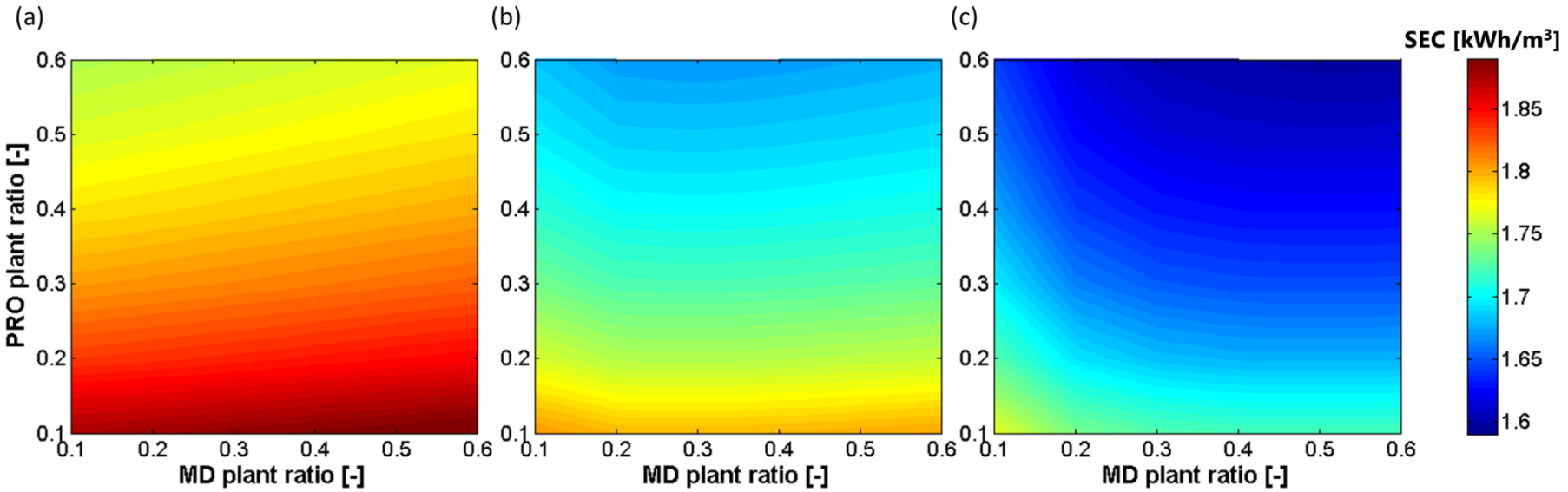
(a)
(b)
(c)
PRO plant ratio [-]
MD plant ratio [-]
MD plant ratio [-]
MD plant ratio [-]
SEC [kWh/m³]
0.1
0.2
0.3
0.4
0.5
0.6
1.6
1.65
1.7
1.75
1.8
1.85

Fig. 6.

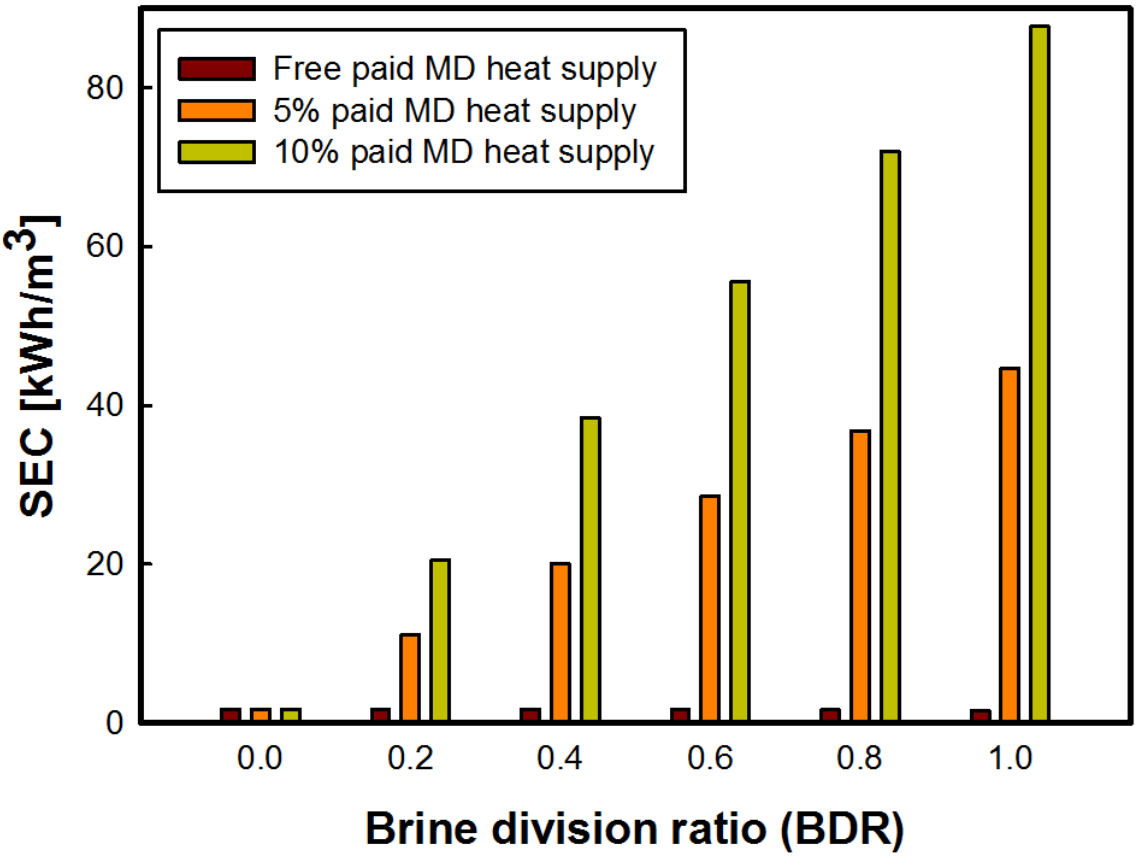

Fig. 7.

Kim *et al.*

Tables captions

Table 1. Simulation conditions.

Table 2. Summary of simulation results (RO influent flow rate: 2000 m^3/d).

Table 3. Sensitivity results of influencing parameters.

Table 1. Simulation conditions.

	Parameter	Value
RO	Channel length	7 (m)
	Channel height	6×10^{-4} (m)
	Channel width	37 × 20 (m)
	Feed concentration	38 (g/L)
	Influent flow rate	2000 (m^3/d)
	Hydraulic pressure	65 (bar)
	Rejection rate	99 (%)
	Temperature	25 (℃)
	PX efficiency	95 (%)
	Number of segments	100
MD	Channel length	7 (m)
	Channel height	6×10^{-4} (m)
	Channel width	37 × 10 (m)
	Feed temperature	60 (℃)
	Permeate temperature	25 (℃)
	Number of segments	100
PRO	Channel length	7 (m)
	Channel height	6×10^{-4} (m)
	Channel width	37 × 10 (m)
	Feed concentration	1.0 (g/L)
	Hydraulic pressure	20 (bar)
	Temperature	25 (℃)
	PX efficiency	90 (%)
	Turbine efficiency	80 (%)
	Number of segments	100

Table 2. Summary of simulation results (RO influent flow rate: 2000 m^3/d).

Parameter	Value
Produced water flow rate	995 (m^3/d)
Recovery rate	49.7 (%)
RO brine flow rate	1005 (m^3/d)
RO brine concentration	76 (g/L)
SEC	1.914 (kWh/m^3)

Table 3. Sensitivity results of influencing parameters.

Parameter	Sensitivity index for SEC	Rank
Cost sharing ratio of MD heat source	1371.2	1
RO hydraulic pressure	1098.6	2
Brine division ratio (BDR)	1001.6	3
RO cross-flow velocity	754.9	4
PRO hydraulic pressure	526.2	5
PRO feed concentration	110.1	6
Plant size ratio of MD and PRO compared to RO	28.16	7